1988A&A...191..303R

Astron. Astrophys. 191, 303–312 (1988)

ASTRONOMY
AND
ASTROPHYSICS

A study of the radio spectral index in the Galactic centre region: evidence for an unusual nonthermal emission component

W. Reich[1], **Y. Sofue**[2,3], **R. Wielebinski**[1], **and J. H. Seiradakis**[1,4]

[1] Max-Planck-Institut für Radioastronomie, Auf dem Hügel 69, D-5300 Bonn 1, Federal Republic of Germany
[2] Nobeyama Radio Observatory*, Tokyo Astronomical Observatory, Minamisaku, Nagano 384-13, Japan
[3] Department of Astronomy, University of Tokyo, Bunkyo-ku, Tokyo 113, Japan
[4] Department of Astronomy, University of Thessaloniki, GR-54006 Thessaloniki, Greece

Received February 13, accepted August 6, 1987

Summary. The distribution of the spectral index in the Galactic centre region has been studied using calibrated maps in the frequency range between 843 MHz and 43.25 GHz. The common angular resolution at three well separated frequencies was 1.′5 which corresponds to 3.7 pc at the Galactic centre distance of 8.5 kpc. We find that flat or slightly inverted spectra are seen in the "Arc" and the "Bridge" region north of Sgr A. After performing a thermal/nonthermal separation we find that most of the nonthermal emission must have a positive spectrum with $\alpha \sim +0.3$ ($S \sim \nu^{+\alpha}$). This unusual emission may be due to electrons with a monoenergetic or low-energy cutoff spectrum. The origin of these particles may be the compact radio source Sgr A* with the same spectral characteristics.

Key words: radio spectral index – Galactic centre – Sgr A

1. Introduction

The Galactic centre region including the strong radio source Sgr A and the extended components often referred to as "Bridge" and "Arc" (Brown and Liszt, 1984) located north of Sgr A, have been the subject of many recent studies at several frequencies. High resolution observations (e.g. Ekers et al., 1983; Lo, 1984; Yusef-Zadeh and Morris, 1987) of Sgr A have shown that it consists of (a) the nonthermal shell structure Sgr A East, often interpreted to be a supernova remnant, (b) the thermal source Sgr A West, located at the western edge of the Sgr A East shell and (c) the extremely compact nonthermal VLBI source Sgr A* embedded within Sgr A West. The source is surrounded by weaker "halo" emission. In contrast to this fairly clear picture of Sgr A, the Bridge and Arc areas have been much harder to observe because of their larger extent, their relative lower surface brightness and complex nature. They both appear to have a flat spectral index but must contain both thermal and nonthermal emission, a conclusion drawn from recombination line observations (Pauls et al., 1976) and polarization measurements (Inoue et al., 1984; Yusef-Zadeh et al., 1984, 1986; Seiradakis et al., 1985; Tsuboi et al., 1985, 1986; Sofue et al., 1987). Bridge and Arc are connected to even larger, weaker structures in the Galactic centre region like the Galactic Centre Lobe (Sofue and Handa, 1984). Its origin is unclear so far, although a flat spectral index is observed for this feature (Sofue, 1985) similar as in the Bridge and Arc area. The accuracy of spectral indices determined so far is low, and only crude estimates could be made for the physical parameters of the emission components.

In this paper we present the results of a thorough spectral index study of the region around the Galactic centre incorporating numerical data from widely separated frequencies (843 MHz, 10.7 GHz, and 43.25 GHz). On this basis we try to separate the thermal from the nonthermal component in this region and to draw conclusions concerning the nature of the emission mechanism. Consistency checks, using published lower frequency data, have also been performed.

2. The data

Radio continuum maps of the Galactic centre region with resolutions better than 1.′5 were published at 843 MHz by Mills and Drinkwater (1984), at 10.7 GHz by Seiradakis et al. (1985) and at 43.25 GHz by Sofue et al. (1986). These data were convolved to the same common resolution of 1.′5 and regridded to the same area of 0.°5 × 0.°55 centred on $\alpha_{1950} = 17^{h}43^{m}$, $\delta_{1950} = -28°54'$. To derive reliable spectral indices we had to adopt a common zerolevel for all maps. This is not trivial, as the interferometric 843 MHz Molonglo data miss large-scale emission, which is clearly visible at 10.7 GHz but is too weak to be seen at 43.25 GHz. A consistent zerolevel was found by means of temperature versus temperature plots (T – T plots) for the area of the Bridge and the northern Arc (see Sect. 3b, Fig. 7 to Fig. 9) and adopted for the whole map. The method of T – T plots, first used by Turtle et al. (1962), allows the determination of the spectral index without the knowledge of absolute intensity levels. In order to adjust all maps to this common zerolevel a flux density of 0.6 Jy/beam area was added to the 843 MHz map and 1 Jy/beam area was subtracted from the 10.7 GHz map, while the 43.25 GHz map was left unchanged. These zerolevel adjustments were

---

Send offprint requests to: R. Wielebinski

* Nobeyama Radio Observatory, a branch of the Tokyo Astronomical Observatory, University of Tokyo, is a facility open for general use by researchers in the field of astronomy and astrophysics

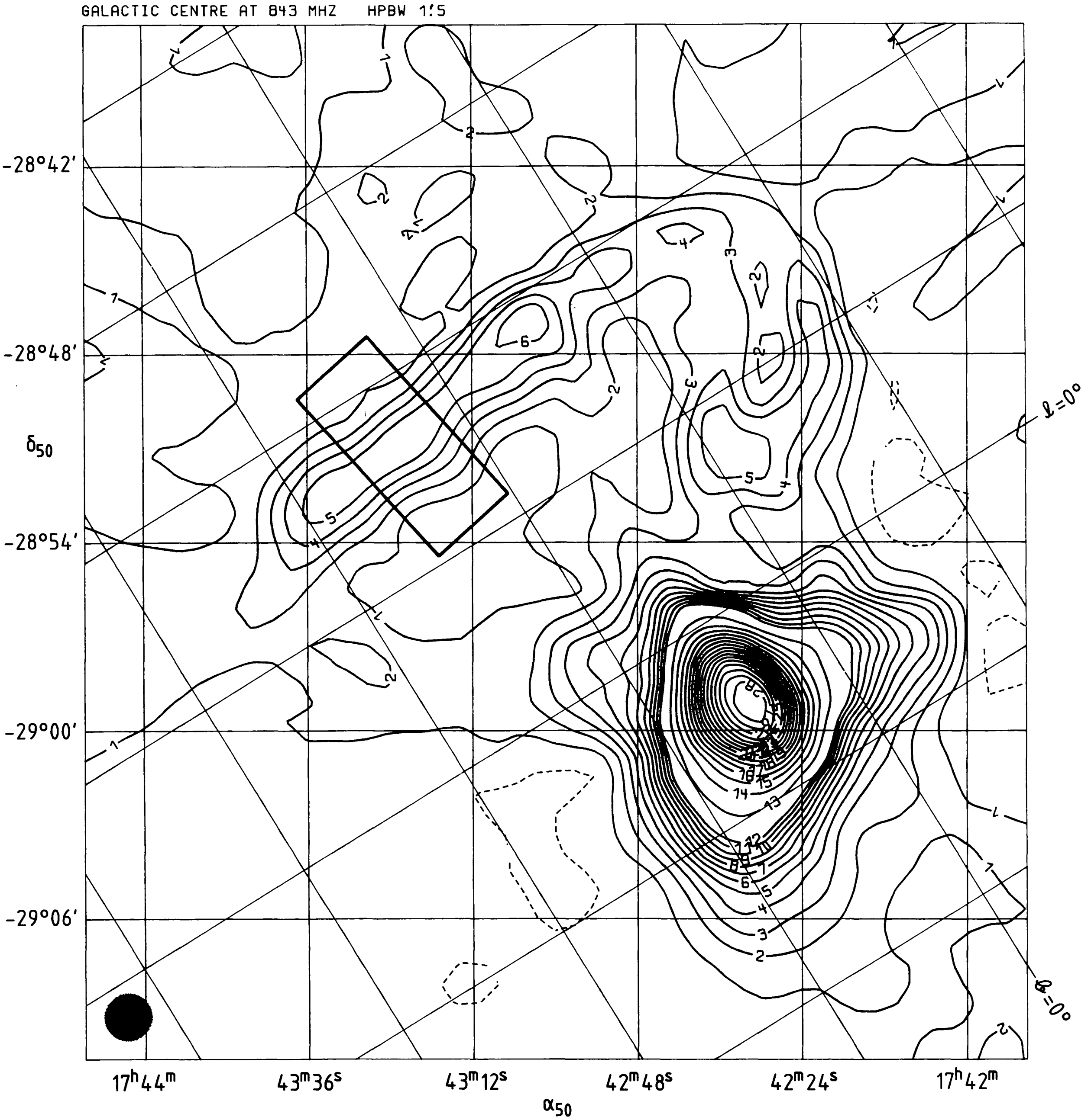

Fig. 1. 843 MHz map of Mills and Drinkwater (1984) convolved to 1.'5. Contours run in steps of 0.5 Jy/beam area from the adopted zero level (dashed) up to 6 Jy/beam area and further in steps of 2.5 Jy/beam area. The box in the Arc region indicates the field where the cross cuts mentioned in the text and shown in Fig. 10 were performed

necessary because the Galactic centre lies in a very hot part of the sky and the regions mapped are not extended enough to have a reasonable zerolevel. The adjustments were based on extended sky surveys of the Galactic centre area (e.g. see Wielebinski, 1987) and the intercepts of the T – T plots in Figs. 7–9. The resulting maps are shown in Figs. 1 to 3. Spectral index maps have been derived between all pairs of maps. We show the results of combining the 843 MHz and 10.7 GHz data in Fig. 4 and that for 10.7 GHz and 43.25 GHz in Fig. 5. In addition, a spectral index map was constructed using a linear fit for the data of all three frequencies, which is shown in Fig. 6.

Because of the large frequency separation any systematic scaling error of a map causes relatively low errors for the derived spectral indices. Even assuming scaling errors as large as +10% for the low-frequency map and −10% for the high-frequency map, the systematic error for the spectral index is $\Delta\alpha = 0.13$ for the closest frequency combination 10.7 GHz/43.25 GHz and $\Delta\alpha = 0.07$ for the largest frequency combination 843 MHz/43.25 GHz. A larger uncertainty of the spectral indices is caused by the relative baseline differences in low-brightness regions. Therefore spectral indices are shown only where the flux density exceeds 1 Jy/beam area at all frequencies used.

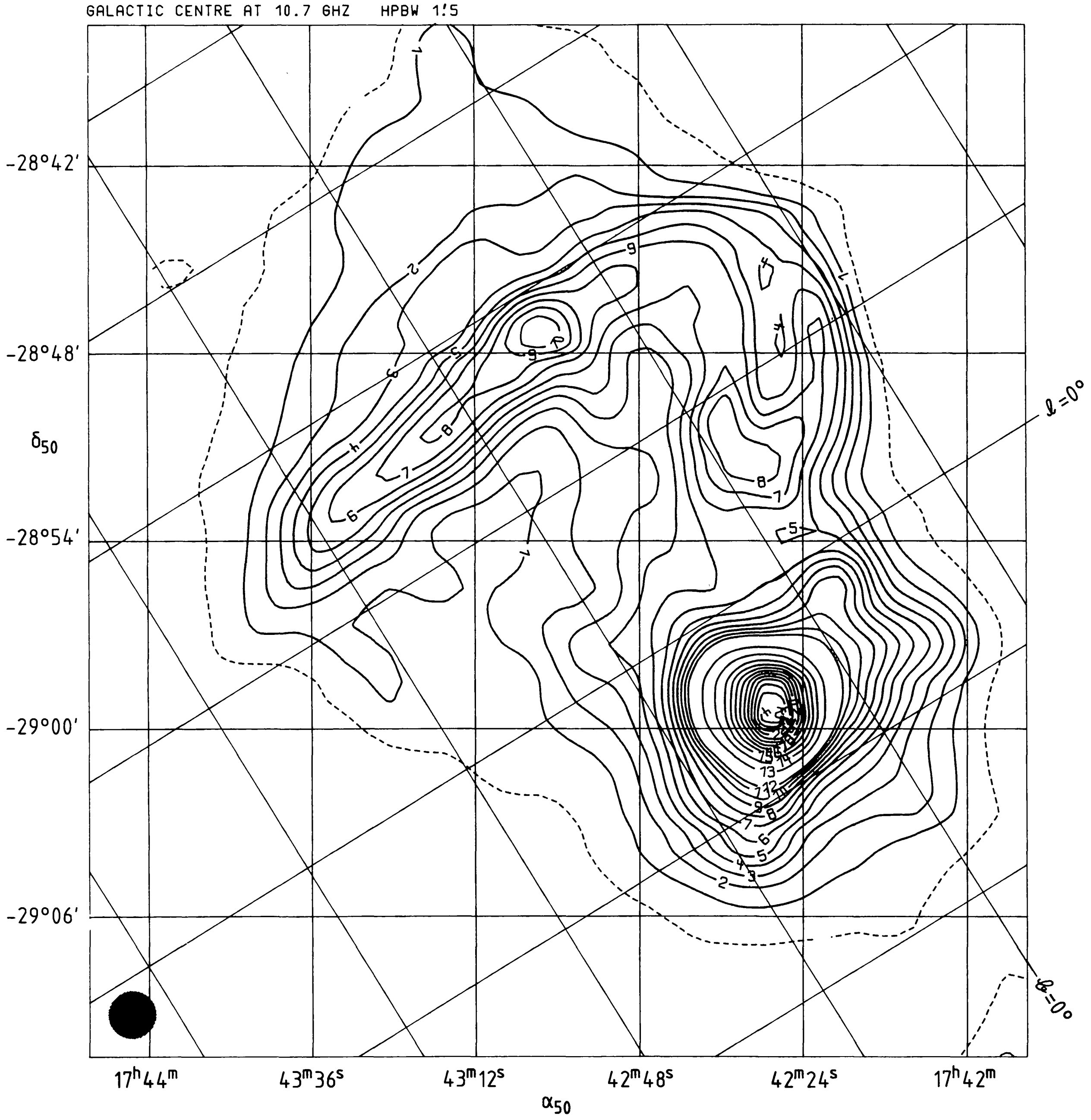

Fig. 2. 10.7 GHz map of Seiradakis et al. (1985) convolved to 1'.5. Contours steps are the same as in Fig. 1

3. Results

In this section we discuss the results of our spectral index investigation for the area around Sgr A, the northern Bridge and the bent Arc region.

3.1. Sgr A

The inner structure of Sgr A remains unresolved at a resolution of 1'.5. The shift of the location of the peak intensity from the 843 MHz map to the high-frequency maps reflects the different positions of the nonthermal shell Sgr A East with steep spectrum and Sgr A West with a thermal emission spectrum. The spectral index map between 843 MHz and 10.7 GHz (Fig. 4) is very similar to that published by Mills and Drinkwater (1984) who used an older 10.7 GHz Effelsberg map (Pauls et al., 1976) for comparison.

Using their own data and data from the literature Mills and Drinkwater (1984) and Sofue et al. (1986) have presented the integrated spectrum of Sgr A. The spectrum seems to be inverted at lower frequencies, showing a bend around 1 GHz and is steep towards higher frequencies with a possible flattening above 50 GHz. Although the general spectral behaviour of Sgr A can be extracted from this composite spectrum, the detailed characteristics could be quite different due to the inhomogeneity of the data used, e.g. different baselevels, sensitivity, integration area, etc. In order to get a more reliable flux density estimate of Sgr A and its

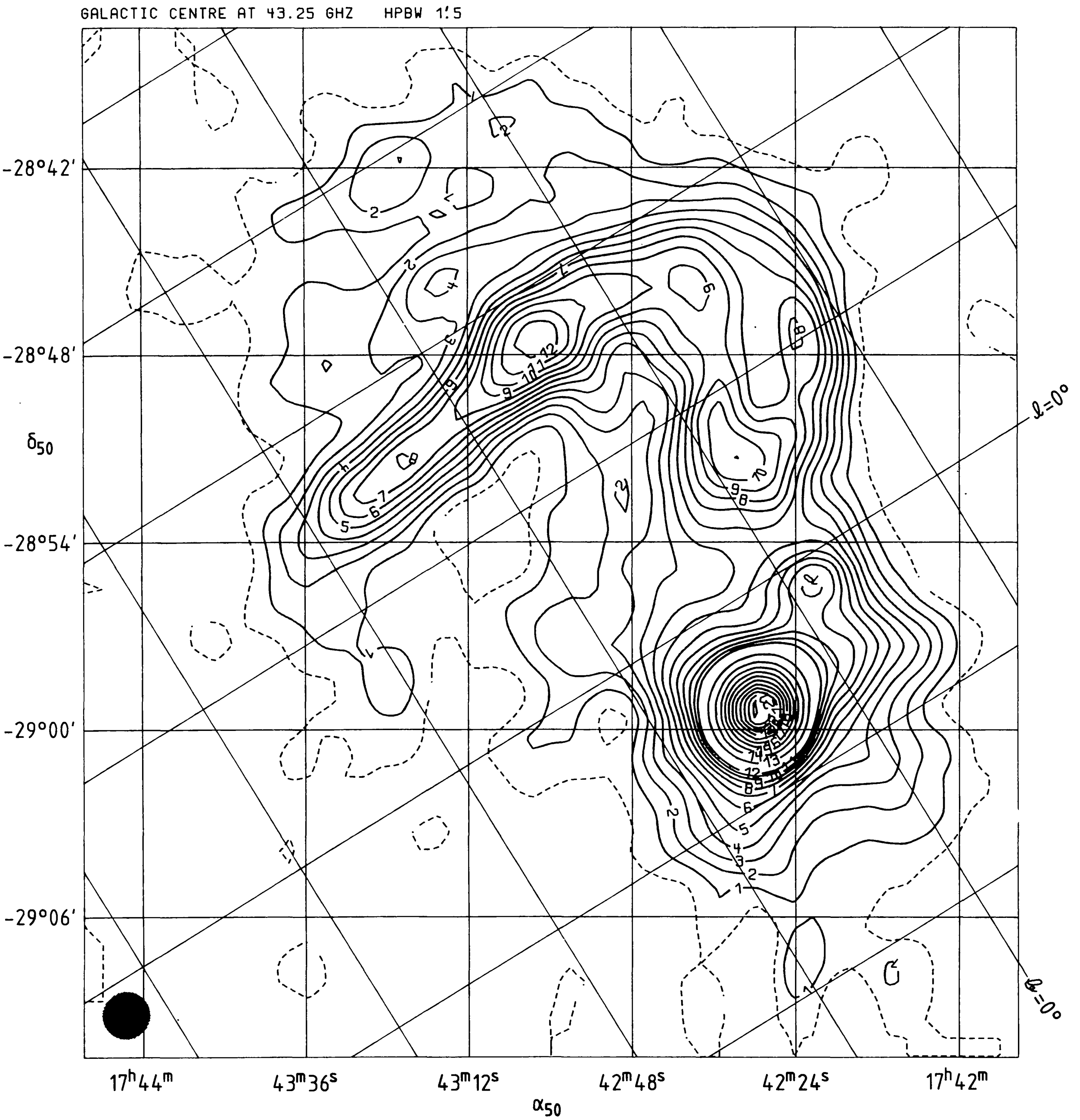

Fig. 3. 43.25 GHz map of Sofue et al. (1986) convolved to 1.′5. Contour steps are the same as in Fig. 1

surrounding area we have performed a ring integration starting from $\alpha_{1950}=17^{\rm h}42^{\rm m}31\overset{\rm s}{.}2$, $\delta_{1950}=-28°58\overset{\prime}{.}8$. The integrated area was limited to $\delta \leqq -28°52\overset{\prime}{.}5$ in order to avoid confusion with the Bridge area. Adopting a relative zerolevel for all frequencies at the integration radius of $7\overset{\prime}{.}5$ from the centre, we derive flux densities as listed in Table 1. Uncertainties of 0.2 Jy/beam area in the determination of the zerolevel result in flux density errors of less than 8%. The integrated spectral index of Sgr A between 843 MHz and 43.25 GHz is $\alpha \sim -0.15$. We made a thermal/nonthermal separation assuming optically thin components with the thermal emission with $\alpha=-0.1$. The result of this decomposition is also listed in Table 1. The nonthermal emission within the $7\overset{\prime}{.}5$ radius has $\alpha=-0.65$ and hence is somewhat above the VLA values of Ekers et al. (1983) for Sgr A East.

3.2. The Bridge area

The extended area ($6\overset{\prime}{.}5\times 6\overset{\prime}{.}5$) centred at $\alpha_{1950}=17^{\rm h}42\overset{\rm m}{.}6$, $\delta_{1950}=-28°48'$, the so-called Bridge area, gives inverted spectral indices for all combinations of maps. However the absolute temperatures are lower compared to the Sgr A area, therefore the spectral index distribution suffers more from zerolevel uncertainties. Using the "T – T plot" method and fitting the slope, we find spectral indices independent of zerolevel offsets. The resulting average spectral index is $\alpha=0.22\pm0.04$ for 843 MHz/10.7 GHz (Fig. 7), $\alpha=0.17\pm0.03$ for 10.7 GHz/43.25 GHz (Fig. 8) and $\alpha=0.20\pm0.03$ for 843 MHz/43.25 GHz (Fig. 9). In order to cross-check our results, we investigated the spectral index distribution in the same area using the 4.75 GHz map shown by

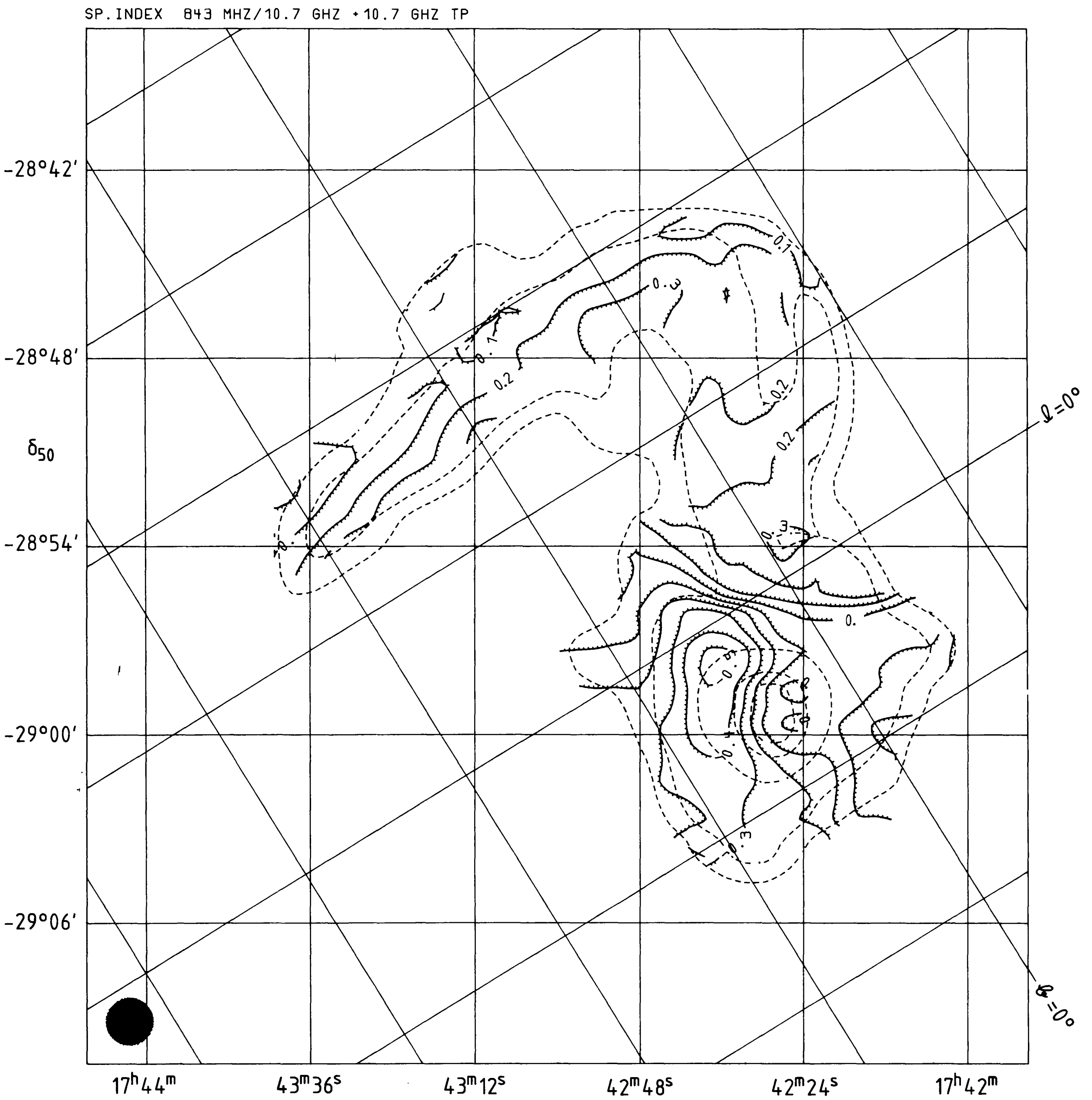

Fig. 4. Distribution of spectral indices α ($S \sim \nu^{\alpha}$) between 843 MHz and 10.7 GHz. Contour steps are 0.1 part with tick marks pointing towards maximum direction. Some total intensity contours from the 10.7 GHz map (Fig. 2) are shown dashed

Sofue et al. (1987) with 2.′4 resolution and the 10.7 GHz map at the same angular resolution. From the T−T plot we obtain an average spectral index of $\alpha = 0.20 \pm 0.11$. All available data indicate in any case an inverted spectrum in this area.

The existence of a thermal component however is well established by detection of recombination lines (Pauls et al., 1976) as well as the existence of a nonthermal component based on polarization measurements (Sofue et al., 1987), Pauls et al. assume the area completely thermal in nature and found electron temperatures between 7000 K and 15000 K. The existence of a nonthermal component will, of course, lower these electron temperatures. Because at frequencies above 10 GHz the thermal gas is always optically thin having a spectral index of $\alpha = -0.1$, the spectral index α of the nonthermal component must be close to $\alpha \sim 0.3$.

Such nonthermal spectra have not been seen in extended Galactic sources so far. Inverted nonthermal spectra are, however, not unusual for the cores of extragalactic radio sources often associated with high variability. If we assume a power law distribution for the relativistic electron energies, then the measured spectral index of $\alpha = 0.3$ corresponds to $\gamma = 0.4 (N(E) \sim \mathrm{E}^{-\gamma}$, where $N(E)$ is the number of electrons with energy E). However, $\alpha = 0.3$ is quite close to a spectral index of $\alpha = 1/3$ expected for synchrotron emission originating in a monoenergetic electron spectrum or a sharp low energy cutoff in the electron spectrum for

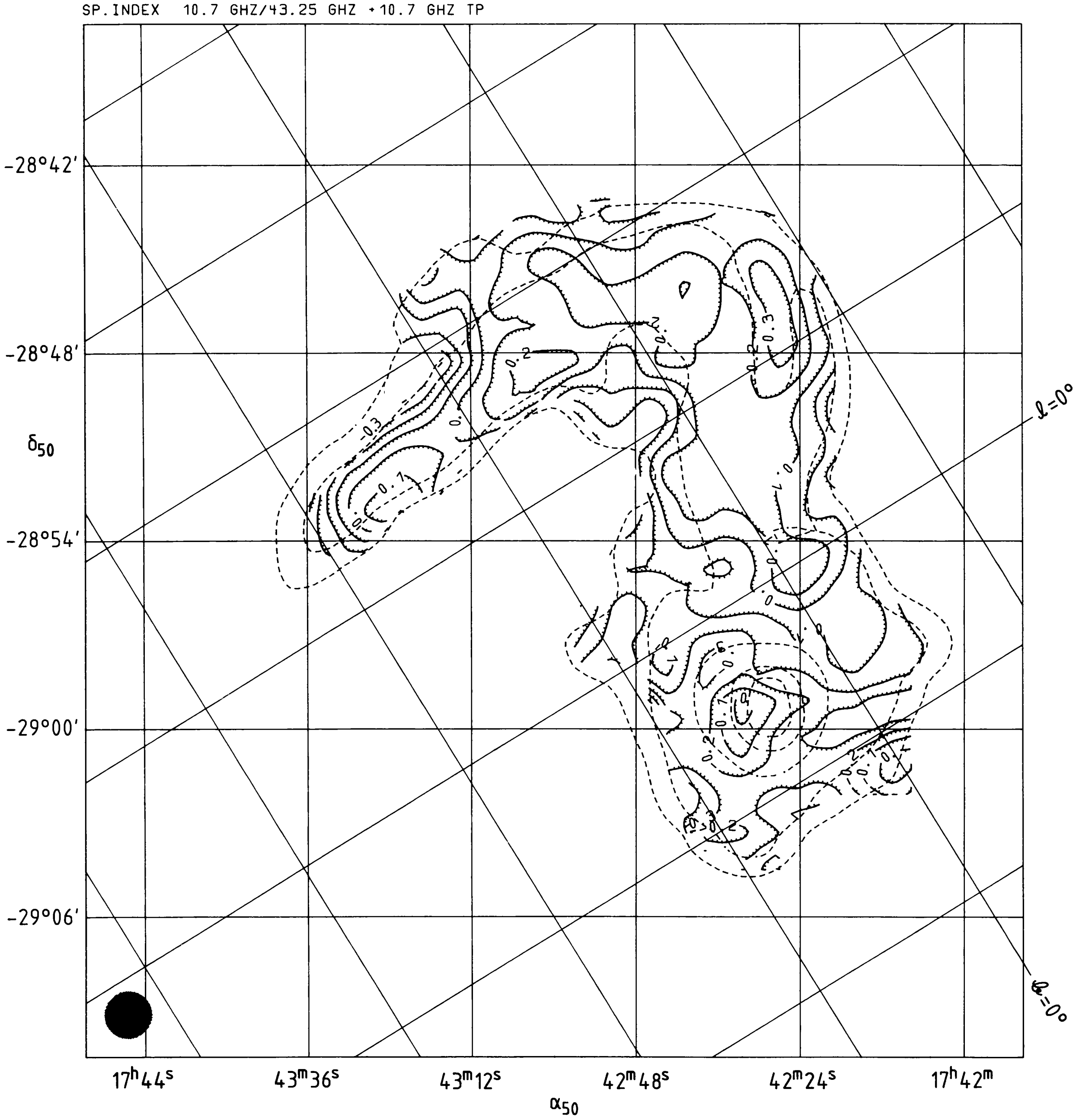

Fig. 5. As Fig. 4, but showing spectral indices between 10.7 GHz and 43.25 GHz

frequencies below the critical frequency ν_c (e.g. Pacholczyk, 1970; Schlickeiser, 1985). If there is a small range of electron energies or the cutoff in the energy spectrum is smooth, α should be somewhat below 1/3.

Assuming the nonthermal spectral index to be $\alpha = 0.3$ we are able to decompose the thermal and nonthermal components for the 10.7 GHz and 43.25 GHz data. With an observed spectral index of $\alpha = 0.17 \pm 0.03$ we obtain 60% for the nonthermal and 40% for the optically thin thermal component at 10.7 GHz. The accuracy is $\pm 10\%$, not including possible scaling errors of the data. A typical thermal fraction of about 40% at 10.7 GHz reduces the electron temperatures T_e obtained by Pauls et al. by 45% ($T_e \sim T_c^{0.87}$, with T_c being the continuum temperature of the thermal emission). The observed range of T_e is now between 3000 K and 6300 K, with a mean temperature near 4500 K.

With $T_e \sim 4500$ K we are able to calculate the expected thermal and nonthermal emission at 843 MHz [assuming a background temperature of 320 K (Mills and Drinkwater, 1984)]. The calculated and observed emission agrees within 10%. However the same calculation for the 408 MHz emission gives about a value 30% less compared with the value derived from the observations of Little (1974). This indicates that the thermal emission is probably a mixture of gas of different temperatures and densities. At very low frequencies (160 MHz) Yusef-Zadeh et al. (1986) discovered radio emission aligned perpendicular to the Galactic plane. Opacities and temperature differences could be mocking an

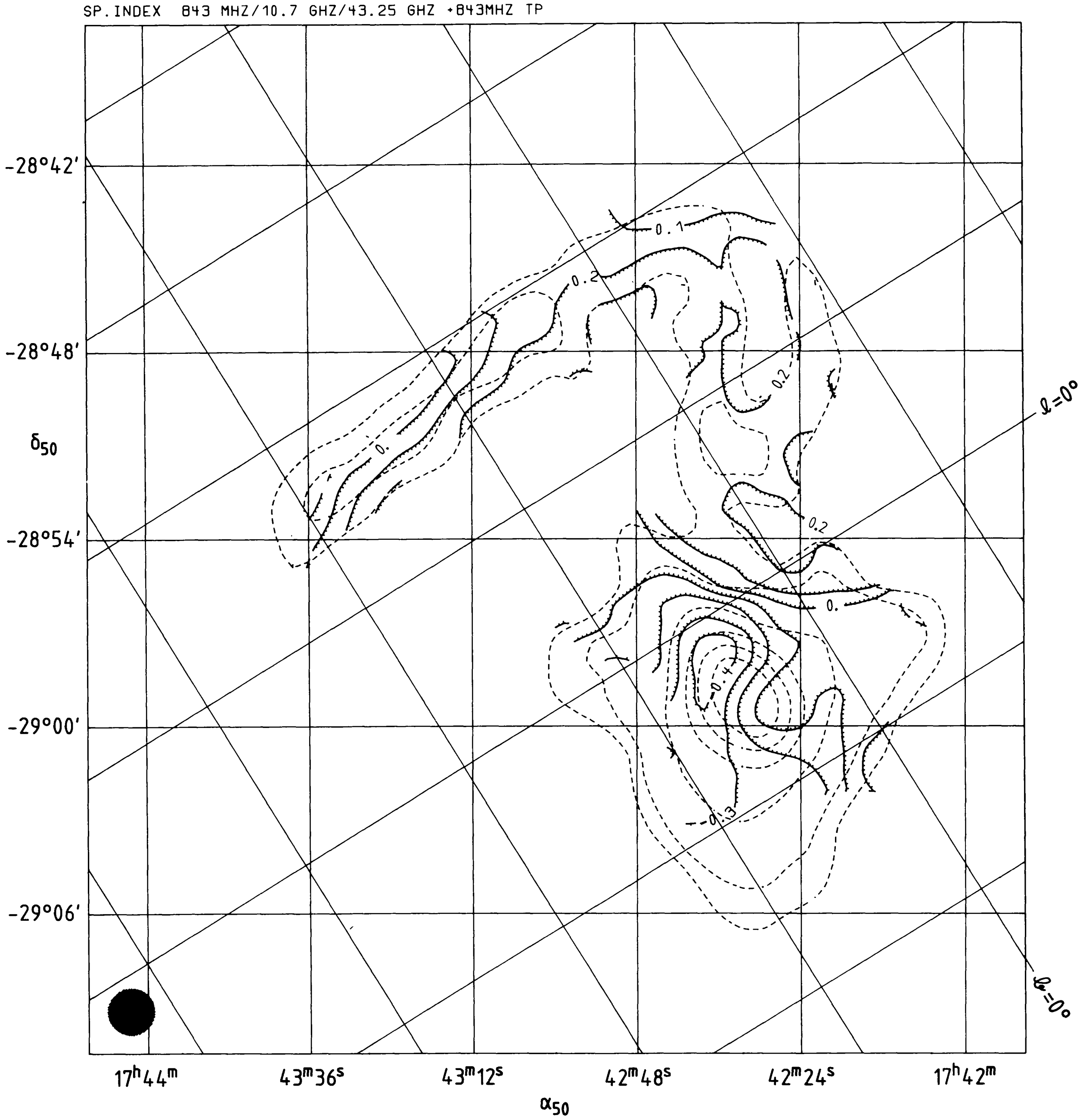

Fig. 6. As Fig. 4, but showing spectral indices between 843 MHz, 10.7 GHz, and 43.25 GHz calculated by a linear fit. Some total intensity contours from the 843 MHz map (Fig. 1) are shown dashed

Table 1. Flux densities of Sgr A (7′.5 integration radius)

Frequency	843 MHz	10.7 GHz	43.25 GHz
Total flux density	303 Jy	197.2 Jy	165.5 Jy
Thermal flux density	238 Jy	184.2 Jy	160.5 Jy
Nonthermal flux density	65 Jy	12.6 Jy	5 Jy

inverted spectrum with thermal gas alone. However, a more accurate fit of the low frequency continuum data requires a knowledge of the distribution, temperature and density of the thermal gas on small scales for the entire field.

The Bridge area has recently been observed with high resolution at 6 cm by Morris and Yusef-Zadeh (1985). They resolved the emission of this area into a number of arched filaments which are believed to be connected with magnetic structures. These filaments also contain thermal gas as shown by high resolution recombination line observations (Yusef-Zadeh, 1986), which may be heated by relativistic electrons.

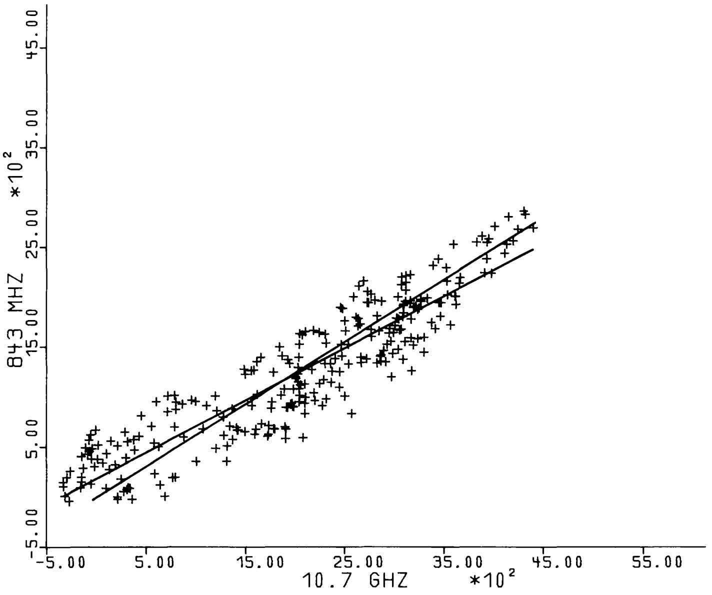

Fig. 7. T – T plot between 843 MHz and 10.7 GHz for the Bridge area. Data are scaled to mJy/beam area. The fitted lines correspond to $\alpha = 0.18$ and $\alpha = 0.26$

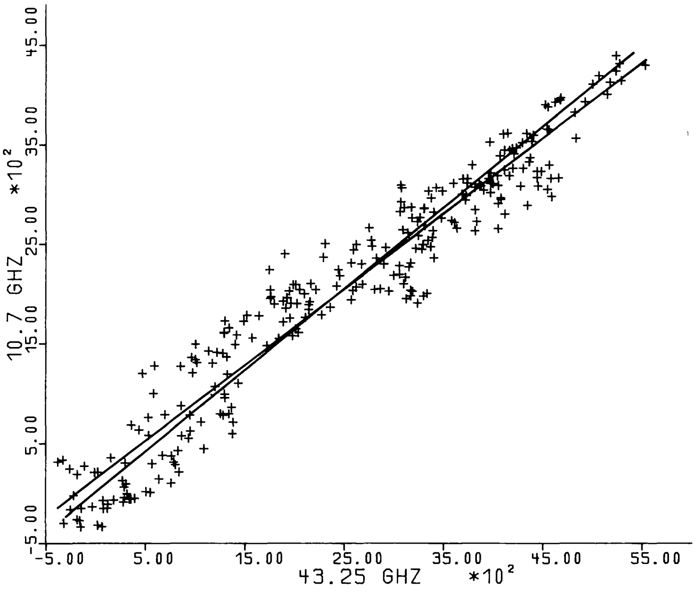

Fig. 8. As Fig. 7 for 10.7 GHz and 43.25 GHz data. The fitted lines correspond to $\alpha = 0.14$ and $\alpha = 0.20$

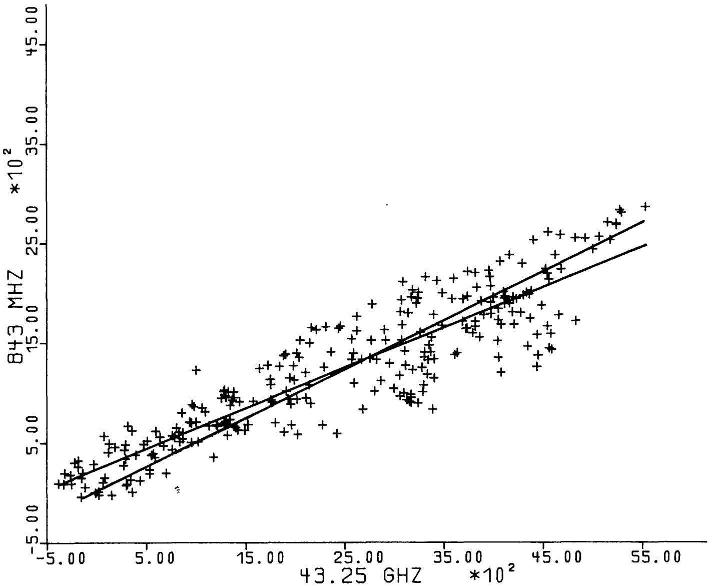

Fig. 9. As Fig. 7 for 843 GHz and 43.25 GHz data. The fitted lines correspond to $\alpha = 0.17$ and $\alpha = 0.23$

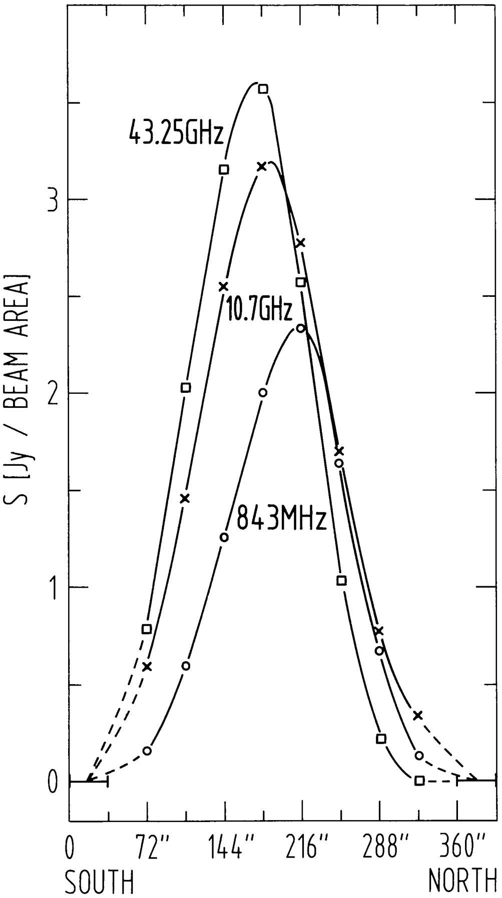

Fig. 10. Average cross cut of the Arc region as obtained by averaging the data at 843 MHz, 10.7 GHz and 43.25 GHz of the field indicated in Fig. 1

3.3. The Arc region

In the Arc region, west of $\alpha_{1950} = 17^{\rm h}43^{\rm m}$ and for $-28\overset{\circ}{.}95 \leqq \delta_{1950} \leqq -28\overset{\circ}{.}75$, no recombination lines have been found, but polarized emission has been detected. This indicates the presence of mainly nonthermal emission, however the high rotation measures found at 5 GHz and 10 GHz (Sofue et al., 1987) imply also the existence of some thermal material in this area. Spectral indices reported so far are flat or slightly inverted (Yusef-Zadeh et al., 1986).

Comparing the position of the maximum intensity along the Arc we note a shift towards lower Galactic longitudes with frequency. This shift is $\approx 40''$ between 843 MHz and 43.25 GHz. Figure 10 shows average cross cuts perpendicular to the ridge for the region marked in Fig. 1 for all three frequencies. A shift of the maximum towards south as well as an increase of intensity with frequency is clearly visible. The high resolution map at 4.9 GHz by Yusef-Zadeh et al. (1986) of this area shows a broad ($\sim 1\overset{\prime}{.}5$) plateau of emission and a superposed narrow ridge ($\sim 20''$) at its southern edge. To explain the intensity variation across the Arc we assume that the southern narrow ridge has the same inverted nonthermal spectrum with $\alpha = 0.3$ as observed in the Bridge region. We obtain a reasonable decomposition if we assume $\alpha = -0.2$ for the broad plateau and an intensity ratio of 5:1 for the narrow and broad component at 43.25 GHz. These assumptions do also account for the intensity ratio of both components seen at 4.9 GHz and the average brightness of ~ 2.5 Jy/beam area at 160 MHz observed by Yusef-Zadeh et al. (1986) in this area.

4. The nonthermal emission in the Bridge and Arc region

Nonthermal extended emission with an inverted spectrum close to $\alpha = 0.3$, as inferred for the Bridge and Arc region, is unusual for Galactic radio sources. As mentioned before the corresponding electron energy spectrum may have a power law distribution $E^{-\gamma}$ with $\gamma = 0.4$, or it is a monoenergetic one, or it has a low-energy cutoff. The question is where such an unusual electron component has its origin. The compact source Sgr A* is unique in the Galaxy and its spectral behaviour [$\alpha \sim 0.2$ up to 115 GHz, Lo (1984)] as seen for the nonthermal emission in the Bridge and Arc region. This is a fairly strong indication that the origin of the particles responsible for this nonthermal emission is the compact source. Kardashev (1985) modelled Sgr A* assuming a quasi-monochromatic energy distribution of particles. He found a much lower magnetic energy than the particle energy within the source. Therefore particles can freely escape. However, for an assumed critical frequency $\nu_c = 10^{12}$ Hz and a source radius $7.5\ 10^{13}$ cm, Kardashev's model gives particle energies of the order of $E \sim 770$ MeV and magnetic field $H_\perp \sim 0.1$ G. These small particle energies cannot account for the extended emission. For the critical frequency limit of $\nu_c \approx 3 \cdot \nu_{\rm max} \approx 200$ GHz set by our observations, the resulting magnetic field strength as given by $\nu_c[\text{MHz}] = 16.1 \cdot H_\perp[\mu\text{G}] \cdot E^2\,[\text{GeV}]$ is $H_\perp \sim 2\ 10^4\,\mu$G. This results in a particle liftime ($t_{1/2}\,[\text{yr}] = 8.352\ 10^9 H_\perp^{-2}\,[\mu\text{G}] \cdot E^{-1}\,[\text{GeV}]$) of ~ 25 yr, which is by far too short compared with the extent of the source of about ~ 30 pc.

However, the source radius is a critical parameter in the model of Kardashev, which was based on older VLBI observations (Geldzahler et al., 1979; Kellermann et al., 1977). More recent observations indicate larger radii of $\sim 1.5\ 10^{14}$ cm or even $\sim 2.5\ 10^{14}$ cm (Lo, 1984; Lo et al., 1985). These values raise the particle energies to ~ 1.5 GeV and give lifetimes of a few hundred years. However recent estimates of the magnetic field strength in the Bridge give $H_\perp \sim 100\,\mu$G (Sofue and Fujimoto, 1987), which requires particle energies of $E \sim 10$ GeV.

Although the numerical estimates are still uncertain, we conclude that the nonthermal emission seen in the Bridge and Arc region is probably connected with the compact source Sgr A*.

5. Conclusion

The results of our spectral index study between 843 MHz and 43.25 GHz of the Galactic centre region can be summarized as follows.

(a) Including its outskirts the spectral index of Sgr A is $\alpha \sim -0.15$. A decomposition into optically thin thermal and nonthermal emission ($\alpha = -0.65$) at 43.25 GHz gives a fraction of 3% for the nonthermal component.

(b) The Bridge region shows an inverted spectrum in the entire frequency range. Decomposition of the emission in a thermal and nonthermal component gives an inverted spectrum for the nonthermal component ($\alpha \sim 0.3$). Along the ridge the nonthermal component is estimated as $\sim 60\%$ at 10.7 GHz. This reduces the electron temperatures deduced from recombination line observations to ~ 4500 K.

(c) In the Arc region the position of maximum emission shifts with frequency towards lower Galactic latitudes and the peak intensity increases with frequency. The emission in this area is known to be nonthermal. The available data can be fitted with a two-component nonthermal spectrum. One component, identified from high-resolution observations with a broad $\sim 1\overset{\prime}{.}5$ ridge of emission, has $\alpha = -0.2$, while a narrow component at the southern edge of the broad feature shows $\alpha = 0.3$ as found for the component in the Bridge region.

(d) The origin of the particles with a $\alpha = 0.3$ spectrum may be Sgr A*, which shows a similar radio spectrum.

Acknowledgements. We thank Prof. B.Y. Mills for making the 843 MHz observations available to us in a machine-readable form and Dr. E. Hummel for critical reading of the manuscript.

References

Brown, R.L., Liszt, H.S.: 1984, *Ann. Rev. Astron. Astrophys.* **22**, 223

Ekers, R.D., van Gorkom, J.H., Schwarz, U.J., Goss, W.M.: 1983, *Astron. Astrophys.* **122**, 143

Geldzahler, B.J., Kellermann, K.I., Schaffer, D.B.: 1979, *Astron. J.* **84**, 186

Inoue, M., Takahashi, T., Tabara, H., Kato, T., Tsuboi, M.: 1984, *Publ. Astron. Soc. Japan* **36**, 633

Kardashev, N.S.: 1985, *Sov. Sci. Rev. E. Astrophys. Space Phys.* **4**, 387

Kellermann, K.I., Shaffer, D.B., Clark, B.G., Geldzahler, B.J.: 1977, *Astrophys. J.* **214**, L 61

Little, A.G.: 1974, in *Galactic Radio Astronomy*, *IAU Symp.* **60**, eds. J.F. Kerr, S.C. Simonson III, 491

Lo, K.Y.: 1984, in *VLBI and Compact Radio Sources*, *IAU Symp.* **110**, eds. R. Fanti, K. Kellermann, G. Setti, p. 265

Lo, K.Y., Backer, D.C., Ekers, R.D., Kellermann, K.I., Reid, M., Moran, J.M.: 1985, *Nature* **315**, 124

Mills, B.Y., Drinkwater, M.J.: 1984, *J. Astrophys. Astron.* **5**, 43

Morris, M., Yusef-Zadeh, F.: 1985, *Astron. J.* **90**, 2511

Pacholczyk, A.G.: 1970, Radio Astrophysics, Freeman, San Francisco, p. 150

Pauls, T., Downes, D., Mezger, P.G., Churchwell, E.: 1976, *Astron. Astrophys.* **46**, 407

Seiradakis, J.H., Lasenby, A.N., Yusef-Zadeh, F., Wielebinski, R., Klein, U.: 1985, *Nature* **317**, 697

Schlickeiser, R.: 1985, in *Active Galactic Nuclei*, ed. F. Dyson, Manchester University Press, 355

Sofue, Y.: 1985, *Publ. Astron. Soc. Japan* **37**, 697

Sofue, Y., Handa, T.: 1984, *Nature* **310**, 568

Sofue, Y., Fujimoto, M.: 1987, *Astrophys. J.* **319**, L73

Sofue, Y., Inoue, M., Handa, T., Tsuboi, M., Hirabayashi, H., Morimoto, M., Akabane, K.: 1986, *Publ. Astron. Soc. Japan* **38**, 475

Sofue, Y., Reich, W., Inoue, M., Seiradakis, J.H.: 1987, *Publ. Astron. Soc. Japan* **39**, 95

Tsuboi, M., Inoue, M., Handa, T., Tabara, H., Kato, T.: 1985, *Publ. Astron. Soc. Japan* **37**, 359

Tsuboi, M., Inoue, M., Handa, T., Tabara, H., Kato, T., Sofue, Y., Kaifu, N.: 1986, *Astron. J.* **92**, 818

Turtle, A.G., Pugh, J.E., Kenderdine, S., Pauliny-Toth, I.I.K.: 1962, *Monthly Notices Roy. Astron. Soc.* **124**, 297

Wielebinski, R.: 1987, in *Mapping the Sky*, *IAU Symp.* **133**, Reidel, Dordrecht (in press)

Yusef-Zadeh, F.: 1986, Ph.D. Thesis, Columbia University, New York

Yusef-Zadeh, F., Morris, M.: 1987, *Astrophys. J.* **320**, 545

Yusef-Zadeh, F., Morris, M., Chance, D.: 1984, *Nature* **310**, 557

Yusef-Zadeh, F., Morris, M., Slee, O.B., Nelson, G.J.: 1986, *Astrophys. J.* **310**, 689